European Review for Medical and Pharmacological Sciences 2021; 25: 3182-3199

LncRNA LINC00958 promotes tumor progression through miR-4306/CEMIP axis in osteosarcoma

Y. ZHOU[1], T. MU[2]

[1]Department of Orthopedics, Beijing Chao-Yang Hospital, Capital Medical University, Beijing, China
[2]Department of Stomatology, Emergency General Hospital, Beijing, China

Abstract. – OBJECTIVE: To investigate the mechanism by which LINC00958 affects osteosarcoma progression through miR-4306/CEMIP axis.

PATIENTS AND METHODS: The microarray data (GSE66673) for gene expression in osteosarcoma cells were obtained from the Gene Expression Omnibus (GEO) database, and differentially expressed genes were analyzed by bioinformatics tools. Real-time quantitative PCR (RT-qPCR) was performed to detect the expression levels of LINC00958, miR-4306, and CEMIP in osteosarcoma tissues and cell lines. Western blot was performed to detect the expression levels of CEMIP. Subcellular fractionation analysis and RNA Fluorescence *in situ* hybridization (FISH) assay were performed to analyze the subcellular localization of LINC00958. The target relationship between LINC00958, CEMIP, and miR-4306 was verified by public bioinformatics database and dual-luciferase reporter assay. RNA immunoprecipitation (RIP) assay was performed to detect LINC00958 and miR-4306 bound to AGO2. The biological functions of LINC00958 and miR-205 on proliferation, cell cycle, apoptosis, migration, and invasion of osteosarcoma cells were evaluated by gain-of-function and loss-of-function experiments. Tumorigenic and metastatic abilities of cells *in vivo* were detected by xenograft tumor experiments and tumor metastasis assays in nude mice. Correlation between miR-4306 and LINC00958 or CEMIP expression in osteosarcoma tissues was analyzed using Pearson correlation analysis. Kaplan-Meier analysis was performed to assess the relationship between LINC00958 expression and overall survival of osteosarcoma patients.

RESULTS: LINC00958 expression levels significantly increased in osteosarcoma tissues while miR-4306 expression levels significantly decreased, and the expression of these two genes was negatively correlated. Subcellular fractionation analysis and RNA FISH assay demonstrated that LINC00958 was mainly localized in the cytoplasm. Dual-luciferase reporter gene assay verified that LINC00958 competitively bound miR-4306 and repressed its expression. Silencing of LINC00958 inhibited proliferation, cell cycle, metastasis, and invasion of osteosarcoma cells while inducing cellular apoptosis. The introduction of miR-4306 inhibitors reversed the tumor-suppressing effect of silencing LINC00958. miR-4306 binds to CEMIP and suppressed its expression. Xenograft tumor experiments and tumor metastasis assays in nude mice demonstrated that silencing LINC00958 inhibited osteosarcoma cells' growth and metastasis while inhibiting miR-4306 reversed this effect. Kaplan-Meier analysis showed that high expression of LINC00958 was significantly associated with poor prognosis of osteosarcoma patients.

CONCLUSIONS: LINC0095 promotes tumorigenesis and metastasis in osteosarcoma by competitively inhibiting miR-4306 expression, leading to elevated expression of CEMIP.

Key Words:
LncRNA LINC00958, MiR-4306, CEMP, Osteosarcoma.

Introduction

Osteosarcoma, also known as osteogenic sarcoma, is one of the most common primary malignant tumors of bone, most often occurring in adolescents under the age of 20 or children[1]. Nearly 60% of all osteosarcoma lesions occur in the distal femur, proximal tibia, femur, and pelvis[2]. Clinically, osteosarcoma is highly malignant, rapidly growing, highly aggressive, and early metastatic[3,4]. Osteosarcoma has the highest mortality and morbidity rate among all types of bone cancer, especially in adolescents[5]. Due to the lack of specificity of clinical symptoms in the early stage of osteosarcoma, the prognosis of

Corresponding Author: Yu Zhou, MD; e-mail: zhouyu2021@126.com

patients is poor, with a 5-year survival rate of 52-56% and a high rate of pulmonary metastasis and recurrence after treatment[6,7]. Therefore, strengthening research on the pathogenesis of osteosarcoma can provide an important basis and reference for clinical diagnosis and treatment.

Long non-coding RNA (LncRNA) is a class of nucleotide fragments whose transcripts are longer than 200 nt without coding capacity, which plays a biological role in embryonic development, cell growth and disease development through splicing regulation, chromatin remodeling and RNA degradation[8-10]. Some studies[11-13] have shown that lncRNAs are often aberrantly expressed in human tumors and are involved in tumor initiation, progression, and metastasis. With the in-depth study of lncRNAs, a large amount of evidence has revealed that the upregulation or downregulation of lncRNAs is closely related to mechanisms such as the development of osteosarcoma[14]. In osteosarcoma cells, elevated expression of lncRNA tends to promote cell proliferation. Liu et al[15] found that LINC01296 expression was elevated in osteosarcoma, while silencing LINC01296 expression inhibited osteosarcoma cell proliferation and induced apoptosis. It was also found that the expression level of cyclin D1 was positively correlated with LINC01296 expression in osteosarcoma tissues, which partly explained the pro-tumorigenic effect of LINC01296 in osteosarcoma. Recent studies have shown that lncRNAs also play an important role in tumor invasion and metastasis. According to Ma et al[16], the expression of FOXF1 and its antisense transcript FOXF1-AS1 (lncRNA) were significantly upregulated in osteosarcoma tissues and cell lines, which were associated with poor prognosis in osteosarcoma patients. Furthermore, silencing FOXF1-AS1 and FOXF1 significantly inhibited osteosarcoma cell migration and invasion *in vitro* and *in vivo* by decreasing the expression of MMP2 and MMP9, whereas enhancing the expression of FOXF1-AS1 had the opposite effect. In this study, LINC00958 was found to be abnormally overexpressed in highly metastatic osteosarcoma cells in the GSE38666 dataset deposited in the GEO database, which prompted us to further define its functional role in the mechanism of osteosarcoma metastasis.

MicroRNAs (miRNAs) are small non-coding RNAs composed of 19-25 nucleotides[17]. miRNAs affect cell proliferation, metastasis, differentiation and apoptosis through complete or incomplete complementary binding to the 3' untranslated region (3'UTR) of target mRNAs, resulting in degradation or translational repression of target mRNAs and negative regulation of gene expression at the post-transcriptional level[18,19]. Some studies indicate that the interaction between lncRNA and miRNA plays a critical role in tumor development. Wang et al[20] found that miR-335 expression was downregulated in osteosarcoma tissues and cell lines and functioned as a tumor suppressor gene. Upregulation of miR-335 can inhibit migration and invasion of osteosarcoma cells by targeting Rho-associated coiled-coil protein kinase 1 (ROCK1). Accumulating evidence suggests that miRNAs regulate a variety of osteosarcoma cell functions, including proliferation, differentiation, metastasis, and apoptosis.

The ceRNA regulatory network is a recently discovered novel mechanism by which RNAs interact with each other *in vivo* and can regulate the action of coding genes, which also extends the previous understanding of the large number of non-coding RNAs *in vivo*[21,22]. Numerous investigations[23,24] have demonstrated that ceRNA networks are widespread in different tumors, and ceRNAs may have an impact on tumor development and prognosis, which could be an indicator for early diagnosis, prognostic evaluation, and a target for cancer therapy. In this study, we identified a long non-coding RNA LINC00958 significantly overexpressed in osteosarcoma tissues and cells and investigated its biological function and mechanism on promoting cell metastasis and invasion in osteosarcoma cells. We found that LINC00958 acts as a ceRNA for miR-4306 and regulates metastasis and invasion of osteosarcoma cells *via* CEMP.

Patients and Methods

Bioinformatics Analysis

The microarray data (GSE66673) for gene expression in osteosarcoma cell was obtained from the GEO database (https://www.ncbi.nlm.nih.gov/geo/), and the parental osteosarcoma cells SAOS-2 and SAOS-2-derived LM5 cells with increased metastatic potential were selected from this microarray study. The parental osteosarcoma cells were used as controls for differential gene expression analysis. Then, background correction and standardized preprocessing were performed using the affy package in the R language, and "limma" package was used for screening dif-

ferentially expressed genes with the screening threshold of | log2FolfChange | > 2.0 and adj.P.Val (the corrected *p*-value) < 0.05[25,26]. The "pheatmap" package was used to construct the differential gene expression heatmap. Next, the downstream miRNAs of LINC00958 were predicted using the RNA22 database (https://cm.jefferson.edu/rna22/) and the starBase 3.0 database (http://starbase.sysu.edu.cn/). Prediction of miRNA target genes was performed using the miRDB database (http://www.mirdb.org/) and the RNA22 database (https://cm.jefferson.edu/rna22/).

Study Samples

Clinical Sample Collection: 63 osteosarcoma cancer tissues and paired normal tissues were collected from 63 patients who received tumor resection in the Department of Oncology of Beijing Chao-Yang Hospital from September 2015 to December 2019. The 63 patients included 34 males and 29 females with a mean age of 20.71± 7.26 years old. All specimens were immediately frozen in liquid nitrogen at -80°C. Patient inclusion criteria: 1) patients were pathologically diagnosed with only osteosarcoma as the primary tumor; 2) patients did not undergo radiotherapy, chemotherapy or biological therapy before surgery; 3) patients had complete clinicopathological and follow-up data. Pathological specimens were confirmed in the Pathology Department, and relevant clinical data were collected through retrospective review of patient files. The detailed parameters of the patients are shown in Table I.

Cell culture: The human normal osteoblast cell line hFOB 1.19, osteosarcoma cell lines HOS, MG-63, U2OS, 143B, and human embryonic kidney cells HEK-293T were purchased from the American Type Culture Collection (ATCC; Manassas, VA, USA). The cells were cultured in Dulbecco's Modified Eagle's Medium (DMEM; Gibco, Grand Island, NY, USA) supplemented with 10% fetal bovine serum (FBS; Gibco, Grand Island, NY, USA), 100 μg/mL penicillin and 100 μg/mL streptomycin in an incubator at 37°C with 5% CO_2. The culture medium was changed every 2 days, and the cells were passaged when they reached about 90% confluence.

Cell Transfection

The sequences of LINC00958, miR-4306, and CEMIP were retrieved from the National Center of Biotechnology Information (NCBI). The design and construction of plasmids for the experiments were based on the pCMV-Flag-N/C vector and entrusted to the Shanghai Sangon Biotechnology Company. The density was adjusted according to the cell growth rate and inoculated in 6-well plates, and the cells were transfected with a density of 80%-90% according to the manufacturer's instructions of lipofectamine 3000 kit (Invitrogen, Carlsbad, CA, USA). Stably transfected cells were selected with G418 (1000 μg/mL) and cultured for 4 weeks after 48 h of transfection. The sequence of sh-LINC00958 were shown as follows: sh-LINC00958-1: 5'-GCAGGCCCAGACCACTTTATA-3, sh-LINC00958-2: 5'-GGC-

Table I. The correlations between lncRNA LINC00958 expression and clinicopathological characteristics in OS patients.

Characteristics	Cases (n)	LINC00958 expression		*p*-value
		High (n = 32)	Low (n = 31)	
Age (years)				0.502
< 18	38	18	20	
≥ 18	25	14	11	
Gender				0.382
Male	34	19	15	
Female	29	13	16	
Metastasis				0.011
Yes	22	16	6	
No	41	16	25	
Tumor location				0.348
Tibia/Femur	39	18	21	
Other	24	14	10	
Enneking stage				0.021
I-IIA	18	5	13	
IIB-III	45	27	11	

CCAGACCACTTTATAAGC-3, sh-LINC00958-3: 5'-GGATCTGTCAGGTTATTTCAT-3.

Reverse Transcription Quantitative PCR (RT-qPCR)

Total RNA was extracted from tissues and cells using TRIzol Reagent (Invitrogen, Carlsbad, CA, USA). Then The total RNA was reversely transcribed into complementary DNA (cDNA) in accordance with the instruction of Primescript™ RT reagent Kit (TaKaRa Biotechnology, Dalian, China) and One Step PrimeScript miRNA cDNA Synthesis Kit (TaKaRa Biotechnology, Dalian, China), respectively. RT-qPCR was performed on an ABI7500 Quantitative PCR instrument (Applied Biosystems, Foster City, CA, USA) using SYBR® Premix Ex Taq™ kit (TaKaRa Biotechnology, Dalian, China). All primers were synthesized by Shanghai Sangon Biotechnology Company, and the primer sequences are listed in Table II. With U6 regarded as an internal reference of miR-4306 and GAPDH as an internal reference of LINC00958 and other genes, the relative expression of products was calculated by the $2^{-\Delta\Delta Ct}$ method. The experiment was repeated three times.

Western Blot Analysis

Total cellular protein was extracted by the RIPA lysis buffer (Solarbio Science & Technology, Beijing, China) supplemented with PMSF. The total protein concentration was measured by BCA kit (Solarbio Science & Technology, Beijing, China) and the sample volume was adjusted to 30 μg protein/lane with deionized water. The samples were subjected to SDS-PAGE gel electrophoresis and transferred onto a polyvinylidene fluoride (PVDF) membrane (Solarbio Science & Technology, Beijing, China). The membranes were blocked with 5% skim milk for 1 h at room temperature and incubated with the anti-CEMIP antibody (Proteintech, Chicago, IL, USA), anti-Cleaved Caspase-3 antibody (Abcam, Cambridge, MA, USA), anti-E-Cadherin antibody (Abcam, Cambridge, MA, USA), anti-N-Cadherin antibody (Abcam, Cambridge, MA, USA) at 4°C overnight. Then the membrane was probed with the horseradish peroxidase (HRP)-labeled goat anti-rabbit immunoglobulin G (IgG) antibody (Proteintech, Chicago, IL, USA) at 37°C for 1 h at room temperature, Subsequently, the bands were visualized using enhanced chemiluminescence (ECL), and these bands were imaged on a Bio-Rad Gel imager (Bio-Rad, Richmond, CA, USA). The gray value was measured using The Image J software and compared with the internal reference to calculate the relative ratio. The experiment was repeated three times.

Fluorescence in Situ Hybridization (FISH)

The FISH probe of LINC00958 was designed and synthesized by Ribobio and labeled with Cy3 fluorescent dye. The RNA FISH assay was performed according to the instructions of the RiboTM lncRNA FISH Probe Mix (Red) kit (Ribobio, Guangzhou, China). Briefly, U2OS and 143B cells cultured on slides were washed with PBS and fixed with 4% paraformaldehyde. They were incubated in 40°C pre-hybridization buffer for 4 h and then hybridized with the probe at 40°C overnight. Afterward, cells were stained with DAPI and imaged with a laser confocal scanning microscope (Leica, Wetzlar, Hesse, Germany).

Subcellular Fractionation Analysis

To determine the cellular localization of LINC00958, nuclear grade fractions were isolated from the cytoplasm according to the instructions of NUCLEI EZ PREP NUCLEI Isolation Kit from the manufacturer (Sigma-Aldrich, St. Louis, MO, USA). The extracted RNA was then subjected to reverse transcription and RT-qPCR. The primer sequences are shown in Table II.

Table II. Primers used in this study.

Primers	Sequence	
	Forward (5′-3′)	Reverse (5′-3′)
LINC00958	CCATTGAAGATACCACGCTGC	GGTTGTTGCCCAGGGTAGTG
miR-4306	AAAGCGCCGCTGGAGAGA	TATGGTTGTTCACGACTCCTTCAC
CEMIP	GCTCTTGAGTTGCATGGACA	ACCGCGTTCAAATACTGGAC
GAPDH	TGGTGAAGACGCCAGTGGA	GCACCGTCAAGGCTGAGAAC
U6	CGCTTCGGCAGCACATATACTA	TCACGAATTTGCGTGTCATCCT

Northern Blot

Total RNA was extracted from U2OS and 143B cells using TRIzol Reagent (Invitrogen, Carlsbad, CA, USA). Northern blot probes for LINC00958 and 18S were prepared by Biotin RNA Labeling Kit (Roche, Basel, Switzerland). After thermal denaturation of total cellular RNA, the RNA samples were separated by formaldehyde denaturing gel electrophoresis and transferred to NC membranes (Solarbio Science & Technology, Beijing, China), which were then incubated with hydration buffer containing the probes. Finally, the RNA signal was detected using a chemiluminescent nucleic acid detection kit (Thermo Fisher Scientific, Waltham, MA, USA).

Dual-Luciferase Reporter Assay

Dual-luciferase reporter assays were used to verify the target relationship between miR-4306 and LINC00958 as well as CEMIP and miR-4306. Luciferase reporter plasmids containing wild-type LINC00958 (wt-LINC00958), mutant LINC00958 (mut-LINC00958), wild-type CEMIP (wt-CEMIP) and mutant CEMIP (mut-CEMIP) were designed and constructed by GenePharma Co., Ltd., (Shanghai, China). The correctly sequenced wild or mutant luciferase reporter plasmids were co-transfected into HEK293T cells with miR-430 mimics or negative control mimics (NC mimic) for 48 h, respectively, and the cells were collected and lysed. According to the manufacturer's instructions, the luciferase activity was determined by the Dual-Luciferase reporter assay kit (Promega, Madison, WI, USA). Fluorescence intensity was measured with a GLomax 20/20 Luminometer fluorescence detector from Promega. The experiment was repeated three times.

RNA Immunoprecipitation (RIP) Assay

The binding of LINC00958 and miR-4306 to AGO2 protein was detected by RIP kit (Millipore, Billerica, MA, USA). Osteosarcoma cells were washed with pre-cooled PBS, and the supernatant was discarded. RIP Lysis Buffer was added, and the products were lysed on ice and collected. Then, the beads were washed with RIP Wash Buffer. After removal of the supernatant, the beads were incubated with 5 μg Argonaute2 (AgO2) antibody (Abcam, Cambridge, MA, USA) for 30 min at room temperature, and normal rabbit immunoglobulin G (Abcam, Cambridge, MA, USA) was used as the control. Subsequently, the cell lysate was incubated with RIP buffer containing magnetic beads. RNA was extracted after proteinase K digestion and used for subsequent RT-qPCR assays.

Cell Proliferation Assay

According to the manufacturer's instructions, cell proliferation capacity was assayed using the Cell Counting Kit-8 (CCK-8, Dojindo, Kumamoto, Japan). Briefly, transfected cells were seeded into 96-well plates at 1×10^4/well and incubated for 24, 48, 72, and 96 h. Subsequently, the absorbance at 490 nm was measured using an enzyme labeling instrument (Bio-Rad, Richmond, CA, USA). The experiment was repeated three times.

Cell Cycle Assay

Flow cytometry analysis was conducted to evaluate the cell cycle. Transfected cells were collected and fixed with 70% ethanol overnight. Subsequently, cells were stained with propidium iodide (PI, Beyotime, Shanghai, China) in the dark for 30 min. Then, the percentage of the cells in G0/G1, S and G2/M phases was detected by flow cytometry (BD Biosciences, Franklin Lakes, NJ, USA). The experiment was repeated three times.

Apoptosis Assay

Cell apoptosis was assessed using Annexin V-FITC/PI Apoptosis Detection Kit (Beyotime, Shanghai, China) according to the manufacturer's instructions. Briefly, transfected cells were harvested and resuspended in binding buffer. Then, Annexin V-FITC (5 μl) and PI (10 μl) were added and incubated for 20 min at room temperature in the dark. Subsequently, the cells were analyzed by flow cytometry (BD Biosciences, Franklin Lakes, NJ, USA). The experiment was repeated three times.

Well Assay

Migration and invasion assays were performed using transwell chambers as described previously. Briefly, U2OS and 143B cells were inoculated in uncoated and Matrigel-coated upper chambers (BD Biosciences, Franklin Lakes, NJ, USA) for migration and invasion assays, respectively. 1×10^5 cells were suspended in serum-free DMEM and inoculated in the upper chamber, and the lower chamber was supplemented with a complete medium containing 10% FBS. After incubation for 24 h, cells were stained with 0.5% crystal violet and photographed under an inverted micro-

scope. Five fields of view were selected at random to count the number of permeating cells under a light microscope and were further analyzed statistically.

Scratch Wound Healing Assay

U2OS and 143B cells were inoculated into 6-well plates at a density of 2×10^5 cells/well, and then replaced with serum-free medium after 100% confluence and scratched vertically with a 200 μl pipette tip. Scratch healing was measured, and the scratch healing rate was calculated.

Animal Model

Female BALB/c nude mice (age: 4-6 weeks; weight: 16-22 g) were provided by the Animal Experimental Center of Beijing Chao-Yang Hospital. The mice were fed with regular food with free access to drinking water in a well-ventilated environment of 50-60% humidity and alternative light/darkness cycle at room temperature. Animal experiments were strictly in line with the Guide for the Care and Use of Laboratory Animal by International Committees. The nude mice were randomly assigned to the following 3 groups (5 mice per group): sh-NC + NC inhibitor (co-delivered with sh-NC and NC inhibitor), sh-LINC00958 + NC inhibitor (co-delivered with sh-LINC00958 and NC inhibitor), and sh-LINC00958 + miR-4306 inhibitor (co-delivered with sh-LINC00958 and miR-4306 inhibitor).

For xenograft tumor experiments, 143B cells with strong growth viability were trypsin digested, resuspended in serum-free DMEM medium and counted. For each group, 1×10^6 cells were suspended in 100 μL serum-free DMEM, and uniformly mixed with 100 μL extracellular matrix (ECM) gel, which was then subcutaneously injected into the back of the nude mice (5 mice per group). After 3 weeks of subcutaneous inoculation, the nude mice were euthanized by carbon dioxide asphyxia, and the tumors were excised and weighed.

For the tumor metastasis assay, 143B cells with strong growth viability were trypsin digested, resuspended in serum-free DMEM medium and counted, and the cell concentration was adjusted to 2×10^7 cells/mL. 100 μL cell suspension was injected into the nude mice through the tail vein. After 30 days of culture, the nude mice were executed and the metastatic foci in the lungs were directly visualized in randomly selected fields.

Hematoxylin and Eosin (HE) Staining

Lung tissues of nude mice were taken and fixed in 10% buffered formalin. Paraffin-embedded tissues were sectioned at 5 mm and stained with HE. Sections were histologically observed and evaluated under light microscopy.

Statistical Analysis

All experimental data were processed and analyzed using SPSS 22.0 statistical software (IBM Corp., Armonk, NY, USA). The measurement data were expressed as mean ± standard deviation. Paired *t*-test was used for the comparison of cancer tissues and adjacent normal tissues, and one-sample *t*-test was used for the comparison between the other two groups. One-way ANOVA was used for comparison between multiple groups, after which pairwise comparisons were made using post hoc tests. Pearson correlation analysis was performed to correlate the expression of LINC00958 and miR-4306 or CEMIP in osteosarcoma tissues. Kaplan-Meier analysis was performed to correlate the high and low expression of LINC00958 in osteosarcoma patients with overall survival (log-rank test). p-value < 0.05 was considered statistically significant.

Results

LINC00958 is Upregulated and Associated with Poor Prognosis in Osteosarcoma Patients

Initially, we retrieved the osteosarcoma cell-based gene expression microarray data (GSE45168) from the GEO database, and the bioinformatics tools were used to perform differential gene expression analysis for osteosarcoma cell. The expression heatmap of the top 25 differentially expressed genes in the datasets is shown in Figure 1A, indicating that long non-coding RNA LINC00958 exhibited significantly higher expression in cells with increased metastatic potential. Therefore, we selected LINC00958 as an important molecule for subsequent analysis. To verify the results from differential expression analysis, we detected the expression of LINC00958 in osteosarcoma tissues and cells by RT-qPCR. The results showed that the expression level of LINC00958 was significantly higher in osteosarcoma tissues compared with corresponding adjacent normal tissues (Figure 1B). The ex-

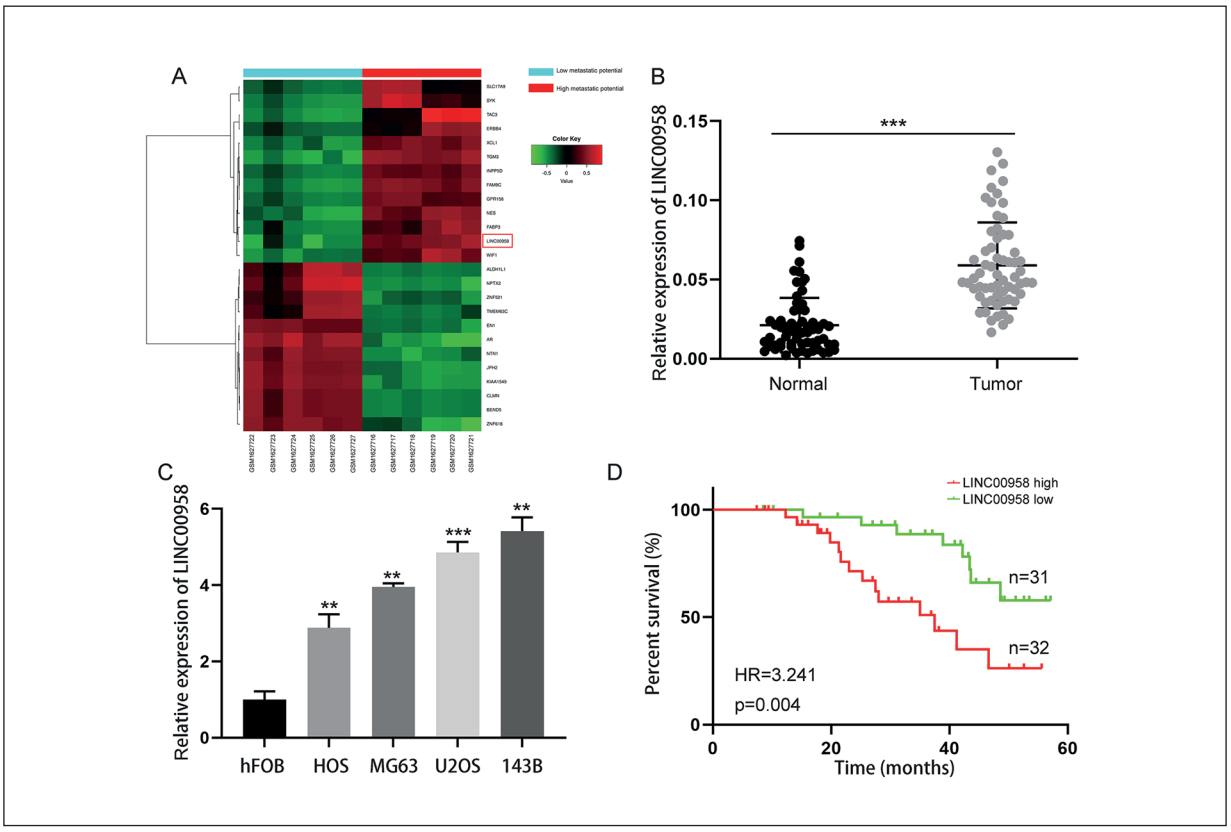

Figure 1. LINC00958 is overexpressed in osteosarcoma and correlates with prognosis. **A,** The expression heat map of the top 25 differential genes in dataset GSE14407. **B,** The expression levels of LINC00958 in osteosarcoma tissues and corresponding adjacent normal tissues were determined by qRT-PCR (n = 63). **C,** The expression levels of LINC00958 in hFOB 1.19, HOS, MG-63, U2OS, and 143B cells was determined by qRT-PCR. **D,** Kaplan-Meier survival curves were used to analyze the correlation between LINC958 expression and overall survival in 63 osteosarcoma patients. Data are represented as mean ± SD. $^{**}p < 0.01$, $^{***}p < 0.001$ *vs.* normal tissues/hFOB 1.19 cell.

pression level of LINC00958 was significantly increased in four osteosarcoma cell lines (HOS, MG-63, U2OS, and 143B) compared with the human normal osteoblast cell line hFOB 1.19, and the expression level of LINC00958 was higher in U2OS and 143B cell lines (Figure 1C). We selected U2OS and 143B cell lines with higher LINC00958 expression for subsequent cell experiments based on the results. To further explore the relationship between the expression level of LINC00958 and the prognosis of osteosarcoma patients, Kaplan-Meier analysis showed that higher expression of LINC00958 was significantly associated with poor prognosis of osteosarcoma patients (HR = 3.241, $p = 0.004$) (Figure 1D). Taken together, the above findings suggested that LINC00958 was expressed at a higher level in osteosarcoma, which was associated with a poor prognosis of osteosarcoma patients.

Biological Characteristics of LINC00958

LINC00958 is annotated as a lncRNA gene in Homo sapiens (NR_038904), located at the p-terminus of chromosome 11 in the genome, and the sequence of LINC00958 is conserved among the mammalian species. First, we detected the presence of LINC00958 in the total RNA of U2OS and 143B cells by Northern blotting experiments (**Supplementary Figure 1A**). To verify the subcellular localization of LINC00958, we isolated the nuclear and cytoplasmic fractions and examined the transcript levels of LINC00958 by RT-qPCR. The results showed that LINC00958 was strongly enriched in the cytoplasmic fraction of both U2OS and 143B cells (**Supplementary Figure 1B**). Besides, we further examined it by RNA fluorescence in situ hybridization assay and obtained consistent results (**Supplementary Figure 1C**). These results strongly suggest that LINC00958 is mainly located in the cytoplasm.

Silencing LINC00958 Inhibits Proliferation, Metastasis, and Invasion of Osteosarcoma Cells While Inducing Cellular Apoptosis

The newly identified lncRNA LINC00958 was upregulated in osteosarcoma tissues and cells. To investigate the effect of LINC00958 on the biological function of osteosarcoma, we examined the effect of LINC00958 on osteosarcoma cells by knocking down or overexpressing LINC00958 in U2OS and 143B cells. The expression level of LINC00958 was verified for both knockdown and overexpression of LINC00958 in osteosarcoma cells compared with control cells (Figure 2A). Sh-LINC00958 target sequences included sh-LINC00958-1, sh-LINC00958-2, and sh-LINC00958-3, among which the first had the highest inhibitory efficiency. Therefore, we chose sh-LINC00958-1 for the subsequent functional experiments (sh-LINC00958 refers to sh-LINC00958-1 in this study). Subsequently, we further investigated the effect of LINC00958 on proliferation, cell cycle, apoptosis, migration and invasion of osteosarcoma cells by gain- and loss-of-function experiments. After LINC00958 knockdown, the proliferation, migration and invasion ability of osteosarcoma cells significantly decreased, while the apoptosis rate and the percentage of G0/G1 phase of the cell cycle significantly increased (Figure 2B-2D, 2F-2H). On the contrary, when LINC00958 was overexpressed by transfection with a plasmid containing the indicated sequence, the proliferation, migration and invasion ability of osteosarcoma cells significantly increased while the apoptosis rate and the percentage of G0/G1 phase of the cell cycle significantly decreased (Figure 2B-2D, 2F-2H). Meanwhile, the expression levels of apoptosis-related proteins (cleaved caspase-3) and epithelial-mesenchymal transition (EMT) related proteins (E-cadherin and N-cadherin) were measured by Western blot assay. The results showed that knockdown of LINC00958 in U2OS and 143B cells increased the abundance of cleaved caspase-3 and E-cadherin and reduced the contents of N-cadherin (Figure 2E, 2I). On the contrary, overexpression of LINC00958 in U2OS and 143B cells reduced the contents of cleaved caspase-3 and E-cadherin and increased the contents of N-cadherin (Figure 2E, 2I). Based on the above results, a conclusion could be drawn that LINC00958 can promote the proliferation, metastasis and invasion of osteosarcoma cells while reducing cellular apoptosis *in vitro*.

LINC0095 Functioned as a Sponge for MiR-195-5p in Osteosarcoma

Recent studies have indicated that many lncRNA play important regulatory roles in a variety of cancers through the competing endogenous RNA (ceRNA) mechanism[27,28]. To determine whether lncRNA LINC00958 regulates gene expression through the ceRNA mechanism, the online bioinformatics software, RegRNA 2.0 and starBase 3.0 were used to predict the downstream miRNAs regulated by LINC00958. The online prediction showed that miR-4306 targets the 3' UTR of LINC00958 (Figure 3A). To determine whether miR-4306 interacts directly with LINC00958, we performed a dual-luciferase reporter assay. The Dual-Luciferase assay results showed that miR-4306 mimic significantly decreased the luciferase activity of LINC00958-Wt; however, the luciferase activity of LINC00958-Mut was not affected by miR-4306 mimic transfection (Figure 3B). Also, RIP assay confirmed that LINC00958 and miR-4306 were both immunoprecipitated by the anti-Ago2 antibody but not by the IgG antibody (Figure 3C), indicating that LINC00958 as a sponge for miR-4306. Then, we further explored the correlation between LINC00958 and miR-4306. LINC00958 downregulation significantly increased the expression level of miR-4306, and conversely, overexpression of LINC00958 evidently decreased the expression level of miR-4306 in U2OS and 143B cells, as revealed by RT-qPCR analysis (Figure 3D). Notably, we also found that miR-4306 expression was down-regulated in osteosarcoma tissues, and the expression of LINC00958 and miR-4306 in osteosarcoma tissues was negatively correlated (Figure 3E and 3D). Taken together, our data demonstrate that LINC00958 acts as a sponge for miR-4306 and negatively regulates miR-4306 expression in osteosarcoma.

MiR-4306 Rescues the Function of LINC00958 in Osteosarcoma Cells

Next, we explored whether the effect of LINC00958 on the biological function of osteosarcoma cells was dependent on the sponging of miR-4306. First, the efficiency of miR-4306 inhibitor was confirmed by RT-qPCR analysis (Figure 4A). Then, rescue experiments were conducted to investigate whether LINC00958 exerted its function through miR-4306 in osteosarcoma cells. After performing the RT-qPCR analysis, the results showed that sh-LINC00958 and NC inhibitor cotransfection significantly increased

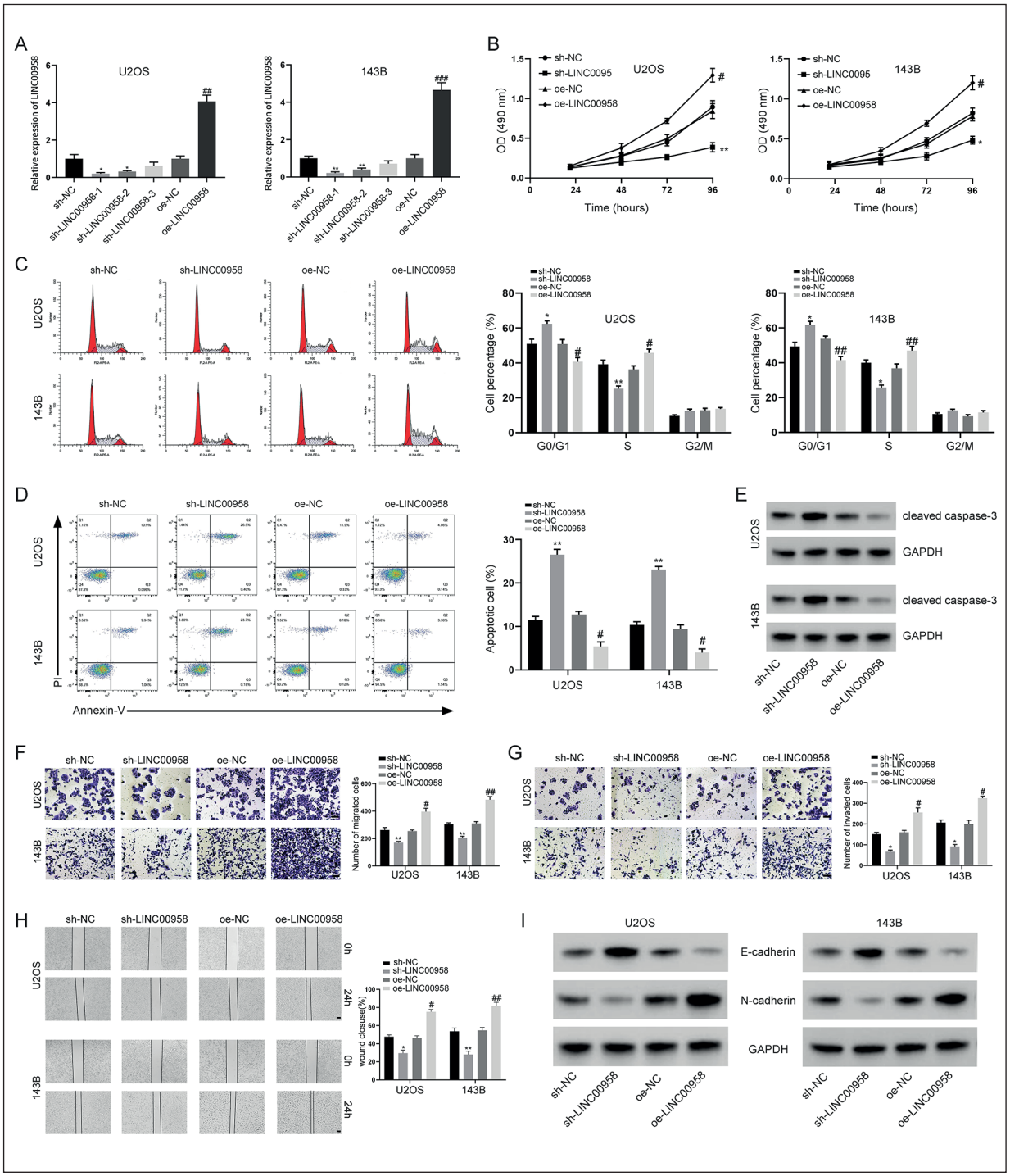

Figure 2. LINC00958 affected the migration and invasion of osteosarcoma cells**. A,** The efficiency of knockdown or overexpression of LINC00958 in U2OS and 143B cells was determined by qRT-PCR. **B,** The proliferation of U2OS and 143B cells was detected by CCK-8 assay. **C,** The cell cycle progression of U2OS and 143B cells was detected by flow cytometry analysis. **D,** Apoptosis rates of U2OS and 143B cells were measured by Annexin V-FITC/PI Apoptosis Detection Kit and analyzed by flow cytometry. **E,** The protein levels of cleaved caspase-3 in U2OS and 143B were assessed by Western blot assay. (**F**) and (**G**) The migration and invasion ability of U2OS and 143B cells evaluated by transwell assay, scale bar = 50 μm. **H,** Scratch wound healing assays were performed to examine the migration capacity of two osteosarcoma cell lines, scale bar = 50 μm. **I,** The protein levels of E-cadherin and N-cadherin in U2OS and 143B cells were assessed by Western blot assay. Data are represented as mean ± SD. *$p < 0.05$, **$p < 0.01$ *vs.* the sh-NC group, #$p < 0.05$, ##$p < 0.01$ *vs.* the oe-NC group.

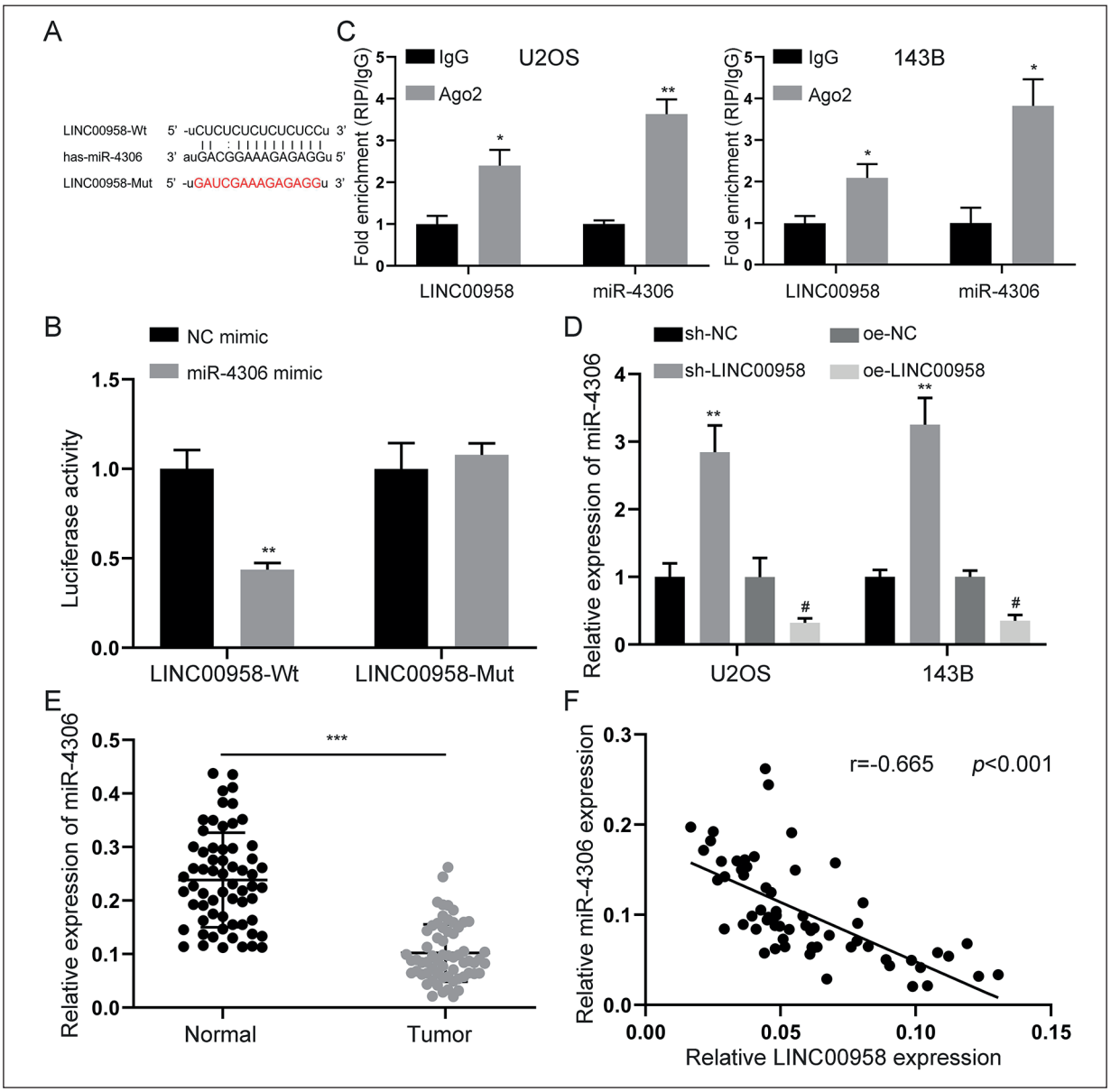

Figure 3. LINC00958 targeted the miR-4306 in osteosarcoma cells. **A,** Schematic representation of the wild-type and mutant binding sites of miR-4306 for LINC00958. **B,** Dual-Luciferase reporter assay was performed to validate the directly targeted role of miR-4306 on LINC00958 in HEK-293T cell. **C,** The interaction of LINC00958, miR-4306 and Ago2 in U2OS and 143B cells were evaluated by RIP assays. **D,** The expression levels of miR-4306 in U2OS and 143B cells were assessed by qRT-PCR after knockdown or overexpression of LINC00958. **E,** The expression levels of miR-4306 in osteosarcoma tissues and corresponding adjacent normal tissues were determined by qRT-PCR (n = 63). **F,** The correlation between miR-4306 and LINC00958 expression in osteosarcoma tissues was measured by Spearman's correlation analysis. Data are represented as mean ± SD. *$p < 0.05$, **$p < 0.01$, ***$p < 0.001$ *vs.* the NC mimic group/the IgG group/the sh-NC group/normal tissues, #$p < 0.05$ *vs.* the oe-NC group.

the expression level of miR-4306 compared with the control group, while these outcomes were abrogated following cotransfection with miR-4306 inhibitor (Figure 4B). Then, functional experiments showed that cells transfected with sh-LINC00958 and NC inhibitor had dramatically suppressed cell proliferation, metastasis and invasion but promoted apoptosis and G0/G1 phase arrest of the cell cycle compared with the negative control; however, miR-4306 inhibitor restored the inhibitory effect of knocking down LINC00958 in 143B and U2OS cells (Figure 4C-4E, 4G-4I). Meanwhile, Western blot assay showed that the abundance of cleaved caspase-3

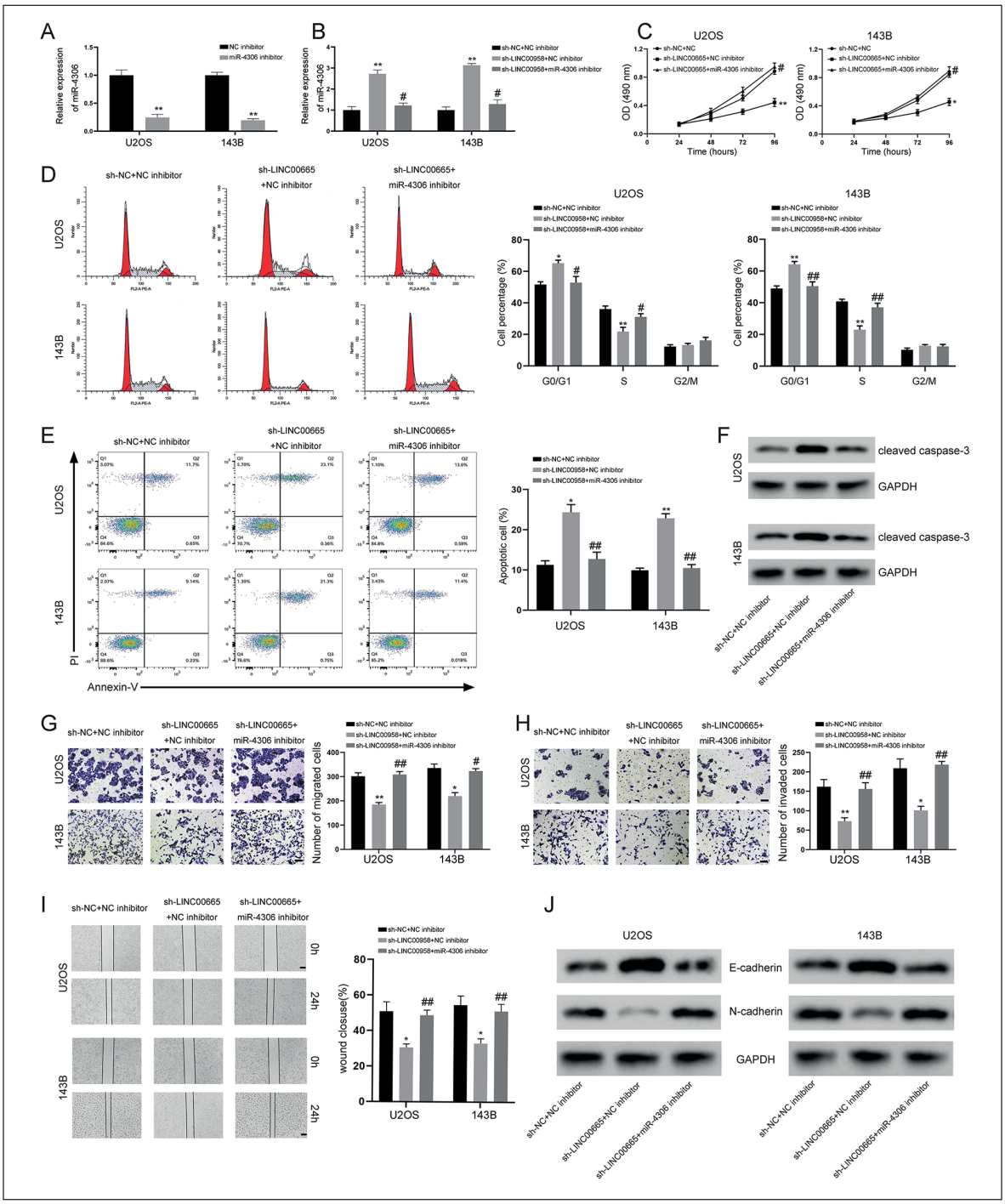

Figure 4. LINC00958 promoted metastasis and invasion of osteosarcoma cells by targeting miR-4306. **A,** MiR-4306 expression in osteosarcoma cells transfected with NC inhibitor or miR-4306 inhibitor was determined by qRT-PCR. **B,** U2OS and 143B cells were cotransfected with sh-LINC00958 and NC inhibitor or miR-4306 inhibitor, and the expression of miR-4306 in the cells was detected by qRT-PCR. **C,** The proliferation of U2OS and 143B cells was detected by CCK-8 assay. **D,** The cell cycle progression of U2OS and 143B cells was detected by flow cytometry analysis. **E,** Apoptosis rates of U2OS and 143B cells were measured by Annexin V-FITC/PI Apoptosis Detection Kit and analyzed by flow cytometry. **F,** The protein levels of cleaved caspase-3 in U2OS and 143B were assessed by Western blot assay. (**G**) and (**H**) The migration and invasion ability of U2OS and 143B cells evaluated by transwell assay, scale bar = 50 μm. **I,** Scratch wound healing assays were performed to examine the migration capacity of two osteosarcoma cell lines, scale bar = 50 μm. **J,** The protein levels of E-cadherin and N-cadherin in U2OS and 143B cells were assessed by Western blot assay. Data are represented as mean ± SD. *$p < 0.05$, **$p < 0.01$ *vs.* the sh-NC + NC inhibitor group, #$p < 0.05$, ##$p < 0.01$ *vs.* the sh-LINC00958 + NC inhibitor group.

and E-cadherin increased, and the contents of N-cadherin decreased in the cells transfected with sh-LINC00958 and NC inhibitor; however, miR-4306 inhibitor restored the inhibitory effect of knocking down LINC00958 in 143B and U2OS cells (Figure 4F, 4J). Our data strongly suggest that LINC00958 exerts an oncogenic effect on osteosarcoma progression by acting as a ceRNA for miR-4306.

CEMIP is a Target of miR-4306 in Osteosarcoma Cells and Positively Regulated by LINC00958

To determine whether the signaling pathways are involved in LINC00958/miR-4306 regulation of osteosarcoma metastasis, we used miRDB and RNA22 to predict potential target genes of miR-4306. Bioinformatics analysis revealed that the 3' UTR sequence of CEMIP is complementary to the seed sequence of miR-4306 and may serve as the functional protein of miR-4306 (Figure 5A). To seek further proof, we used a Dual-Luciferase reporter assay to verify the above prediction. The results showed that the expression of CEMIP-Wt-driven luciferase cotransfected with miR-4306 mimics was significantly reduced compared with the control, but this inhibition was abolished by mutation of the putative miR-4306 binding site in the 3' UTR of CEMIP (Figure 5B). Besides, to confirm whether CEMIP is directly regulated by miR-4306, we measured the mRNA and protein levels of CEMIP upon miR-4306 overexpression in U2OS and 143B cells. We found that both mRNA and protein levels of CEMIP were significantly reduced after overexpression of miR-4306 (Figure 5C and 5D). Subsequently, the expression of CEMIP in osteosarcoma tissue samples and corresponding adjacent normal tissues was examined by RT-qPCR. The results showed that the expression of CEMIP at the mRNA level was significantly higher in osteosarcoma tissues compared with corresponding adjacent normal tissues (Figure 5E). Interestingly, Spearman correlation analysis further showed a negative correlation between miR-4306 and CEMIP mRNA levels in osteosarcoma tissues (Figure 5F). Collectively, these experiments identified CEMIP as a direct target of miR-4306 in osteosarcoma cells.

Since LINC00958 can sponge miR-4306, we next determined whether LINC00958 can regulate CEMIP expression. We found that knockdown of LINC00958 significantly reduced CEMIP protein levels in U2OS and 143B cells (Figure 5G). To determine whether miR-4306 plays a role in the relationship between LINC00958 and CEMIP, we investigated the expression levels of CEMIP in cells co-transfected with sh-LINC00958 and miR-4306 inhibitors. Indeed, the inhibitory effect of knocking down LINC00958 on CEMIP was partially blocked by the miR-4306 inhibitor (Figure 5H). Therefore, the results suggest that LINC00958 positively regulates CEMIP expression in osteosarcoma cells through sponge miR-4306.

Silencing LINC00958 Inhibits Osteosarcoma Cell Tumorigenesis and Metastasis In Vivo

In the above study, we found that LINC00958 targeting miR-4306 /CEMIP axis regulates the progression of osteosarcoma *in vitro*. To further investigate the effects of LINC00958 and miR-4306 on osteosarcoma growth and metastasis *in vivo*, xenograft models and lung metastasis models were established by subcutaneous or tail vein injection of 143B cells with different genetic modifications in nude mice, respectively. Xenograft model showed that the weight of tumors was significantly reduced in the sh-LINC00958 + NC inhibitor group compared with the control group, while co-transfection with miR-4306 inhibitor partially rescued the inhibitory effect on tumor growth (Figure 6A). Lung metastasis models showed that the number of macroscopically visible pulmonary metastatic nodules in the lungs of the sh-LINC00958 + NC inhibitor group was significantly reduced compared with the control group. Similarly, co-transfection with miR-4306 inhibitor partially restored the inhibitory effect on tumor metastasis (Figure 6B). Subsequently, lung tissue sections were prepared and examined after hematoxylin and eosin staining, and the differences in the number of intrapulmonary microscopically visible pulmonary metastatic nodules between groups were consistent with the above conclusion (Figure 6C). These data strongly suggest that LINC00958 has a key role in promoting osteosarcoma genesis and metastasis *in vivo* via the miR-4306 /CEMIP axis.

Discussion

Osteosarcoma is the most common malignancy that occurs in children and adolescents[2]. Although the development of new clinical adjuvant chemotherapeutic agents has greatly alleviated the pro-

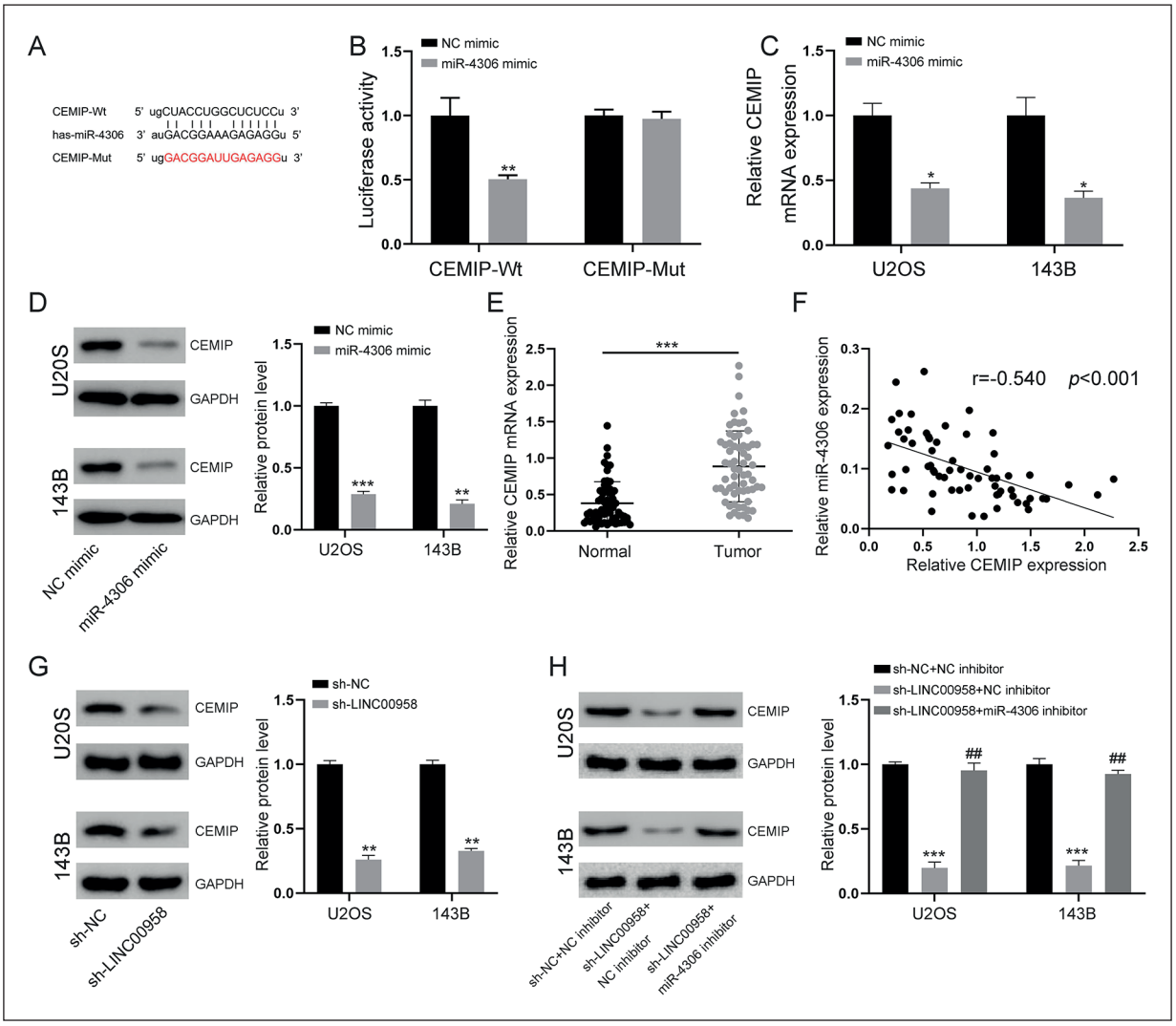

Figure 5. LINC00958 promoted CEMIP expression in osteosarcoma cells by inhibiting miR-4306. **A,** Schematic representation of the wild-type and mutant binding sites of miR-4306 for CEMIP. **B,** The binding of miR-4306 and CEMIP mRNA verified by dual-luciferase reporter assays in HEK-293T cell. **C,** The expression of CEMIP mRNA in osteosarcoma cells transfected with NC mimic or miR-4306 mimic was determined by qRT-PCR. **D,** The protein levels of CEMIP in U2OS and 143B cells were assessed by Western blot assay. **E,** The expression levels of CEMIP mRNA in osteosarcoma tissues and corresponding adjacent normal tissues was determined by qRT-PCR (n = 63). **F,** The correlation between miR-4306 and CEMIP mRNA expression in osteosarcoma tissues was measured by Spearman's correlation analysis. **G,** The expression of CEMIP protein in osteosarcoma cells transfected with sh-NC or sh-LINC00958 was determined by Western blot assay. **H,** U2OS and 143B cells were cotransfected with sh-LINC00958 and NC inhibitor or miR-4306 inhibitor, and the expression of CEMIP in the cells determined by Western blot assay. Data are represented as mean ± SD. $*p < 0.05$, $**p < 0.01$, $***p < 0.001$ *vs.* the NC mimic group/normal tissues/the sh-NC group/the sh-NC + NC inhibitor group, $\#\#p < 0.01$ *vs.* the sh-LINC00958 + NC inhibitor group.

gression of osteosarcoma patients[29,30], malignant metastasis remains a major cause of treatment failure in osteosarcoma patients[31]. Therefore, it is necessary to probe into the molecular mechanism of osteosarcoma development and explore new therapeutic strategies and methods to break the bottleneck of osteosarcoma treatment. With the continuous development of molecular biotechnology, researchers have found that lncRNAs play important regulatory roles in a variety of biological processes, and abnormally expressed lncRNAs may be involved in the development of multiple human diseases, especially in malignant tumors like osteosarcoma[14,32-34]. We found that lncRNA LINC00958 was markedly upregulated and significantly associated with poor survival in osteosarcoma patients. Mechanistic studies further showed that LINC00958 functions as ceRNA

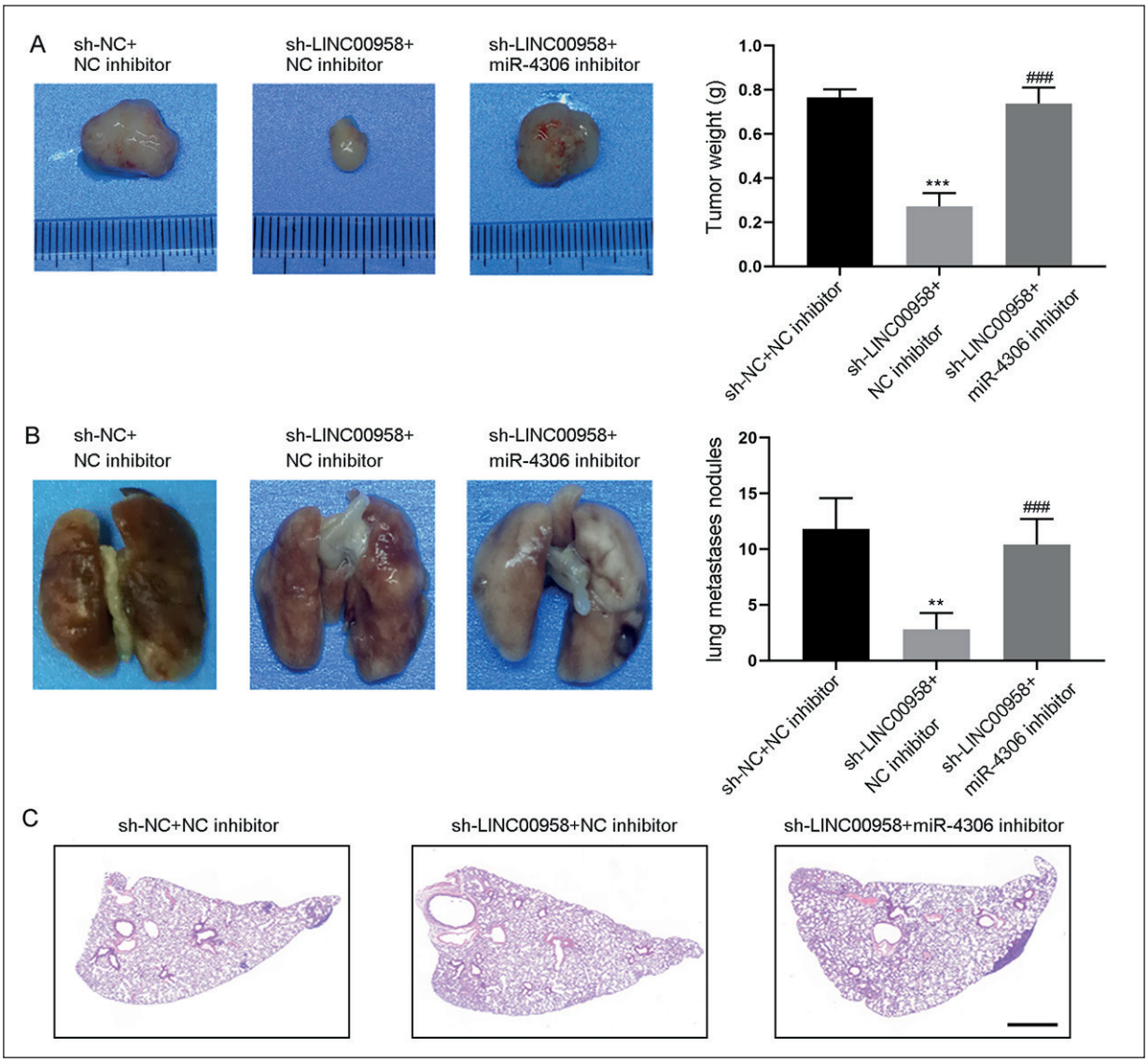

Figure 6. LINC00958 promoted osteosarcoma growth and metastasis by regulating miR-4306 *in vivo*. **A,** Representative images of subcutaneous xenograft tumors *in vivo* and the final tumor weight of each group. **B,** Representative images of metastatic lung nodules and quantitation of metastatic lung nodules after intravenous injection of 143B cells in the whole lung. **C,** Representative HE analysis of sections of lung metastases from mice injected with 143B cells, scale bar = 1000 μm. Data are represented as mean ± SD. $^{**}p < 0.01$, $^{***}p < 0.001$ *vs.* the sh-NC + NC inhibitor group, $^{###}p < 0.001$ *vs.* the sh-LINC00958 + NC inhibitor group.

to sponge miR-4306, leading to increased CEMIP expression and thus promoting osteosarcoma cell tumorigenesis and metastasis *in vitro* and *in vivo*. It is suggested that LINC00958 plays an oncogenic role in the development of osteosarcoma and can be used as a prognostic indicator for osteosarcoma patients.

Currently, an increasing number of studies have identified functional lncRNAs, previously referred to as "junk RNAs", that regulate a variety of osteosarcoma pathological processes such as development, metastasis, and invasion[35,36]. We found that LINC00958 promotes the migration and invasion of osteosarcoma cells *in vitro* and distant lung metastasis *in vivo*. To our knowledge, the present study is the first to report that LINC00958 regulates osteosarcoma cell metastasis. Notably, in lymph node metastatic bladder cancer, the expression of LINC00958 (also named bladder cancer-associated transcript 2, BLACAT2) was significantly upregulated and associated with lymph node metastasis. Overex-

pression of LINC00958 promoted bladder cancer-associated lymphatic vessel generation and lymphatic metastasis[37]. Besides, the researchers observed abnormally elevated expression of LINC00958 in lung adenocarcinoma (LUAD). The tumorigenic properties of LINC00958 in LUAD were revealed by reversing the inhibitory effect of LINC00958 on LUAD cell proliferation, migration, and invasion[38]. These findings further support the potential pro-oncogenic role of LINC00958 in tumorigenesis development. However, the molecular mechanisms underlying the pro-oncogenic role of LINC00958 in human tumors, including osteosarcoma, have not been fully elucidated.

Since 2007, the first ceRNA hypothesis was proposed that the non-protein-coding transcript of IPS1 increases PHO2 mRNA by complementarily binding to miR-399, which has attracted significant global interest in deciphering the underlying mechanism[39]. Some scholars[40,41] support the existence of a novel and extensive interaction network involving ceRNAs, in which lncRNAs regulate the level of protein-coding mRNA molecules by competitively binding miRNAs. For example, MT1JP acts as a ceRNA that competitively binds to miR-92a-3p and upregulates the expression of FBXW7 to regulate gastric cancer progression[42]. In addition, LINC00958 acts as a sponge for miR-330-5p in pancreatic cancer and promotes PAX8-mediated tumor cell growth, invasion and metastasis[43]. Interestingly, in our study, FISH and subcellular fractionation analysis revealed that LINC00958 was located in the cytoplasm of osteosarcoma cells, which made it likely to function as a ceRNA. Next, we further explored the molecular mechanisms by which LINC00958 regulates the metastasis and invasion of osteosarcoma cells. Bioinformatics analysis and *in vitro* experimental studies revealed that LINC00958 negatively regulates miR-4306 expression through complementary binding sites. Moreover, cellular experimental studies revealed that miR-4306 inhibitor antagonized the anticancer effect induced by LINC00958 knockdown. These data demonstrate that LINC00958 exerts oncogenic effects by downregulating miR-4306 expression, suggesting that miR-4306 is an important tumor suppressor gene in the process of metastasis and invasion in osteosarcoma. In conclusion, LINC00958 may act as a ceRNA to regulate the proliferation, cell cycle, apoptosis, metastasis, and invasion of osteosarcoma cells by targeting miR-4306.

In general, lncRNAs function as ceRNAs in different ways to influence intracellular signaling and cell fate, which are largely dependent on miRNA targets[44]. Then, we predicted CEMIP as a potential target of miR-4306 using an online database and further verified the prediction by a dual-luciferase reporter gene assay. Furthermore, cellular experiments demonstrated that overexpression of miR-4306 or knockdown of LINC00958 significantly inhibited the expression of CEMIP protein. CEMIP, also known as KIAA1199, is localized at 15q25.1 and encodes a protein of approximately 150 kDa, which was identified as a novel protein involved in hyaluronan degradation[45,46]. Recent studies[47,48] have shown that CEMIP is expressed in a variety of tissues and that its expression is abnormally high in tumor tissues and is strongly associated with tumor metastasis and invasion, progression, and prognosis. For example, Zhao et al[49] revealed microtubule destabilization regulated by KIAA1199 through the PP2A/stathmin pathway, which in turn promotes metastasis in colorectal cancer cells, while Shen et al[50] found that CEMIP may promote ovarian carcinogenesis and progression through activation of the PI3K/AKT signaling pathway. In our study, we demonstrated that LINC00958 upregulated CEMIP expression by competitively sponging miR-4306, which promoted osteosarcoma tumorigenesis and metastasis accordingly.

In summary, we comprehensively investigated the functional role and molecular mechanisms of LINC00958 in osteosarcoma. Our results showed that LINC00958 expression was upregulated in osteosarcoma cell lines and tissues. Higher expression of LINC00958 was significantly associated with poor prognosis in osteosarcoma patients. Functional and mechanistic analyses indicated that LINC00958 increases the expression level of CEMIP by acting as a ceRNA for miR-4306, which in turn promotes the tumorigenesis and metastasis of osteosarcoma cells *in vitro* and *in vivo*. Therefore, we suggest that LINC00958 could be both a significant marker for the prognosis of osteosarcoma patients and an important target for osteosarcoma gene therapy.

Conclusions

We observed that the expression of LINC00958 is markedly elevated in osteosarcoma and is significantly associated with metastasis and

poor prognosis of osteosarcoma. In addition, LINC00958 may promote malignant progression of osteosarcoma by regulating the miR-4306/CEMIP axis.

Conflict of Interest

The Authors declare that they have no conflict of interests.

Funding

The work was funded by the Teaching Research and Reform Foundation of Gansu University of Chinese Medicine (YBXM-16).

Availability of Data and Materials

The datasets and supporting materials generated during and/or analyzed during the current study are available from the corresponding author on reasonable request.

Ethics Approval and Consent to Participate

The whole study was approved by the Ethics Committee of Beijing Chao-Yang Hospital. All animal research was carried out following the Declaration of Helsinki. Written informed consent was obtained from all patients.

Authors' Contribution

Y Zhou designed the study, conducted the experiments and drafted the manuscript. T Mu collected and analyzed the data. All authors read and approved the final manuscript.

References

1) Taran SJ, Taran R, Malipatil NB. Pediatric osteosarcoma: an updated review. Indian J Med Paediatr Oncol 2017; 38: 33-43.
2) Ferguson JL, Turner SP. Bone cancer: diagnosis and treatment principles. Am Fam Physician 2018; 98: 205-213.
3 Hadjimichael AC, Foukas AF, Savvidou OD, Mavrogenis AF, Psyrri AK, Papagelopoulos PJ. The anti-neoplastic effect of doxycycline in osteosarcoma as a metalloproteinase (MMP) inhibitor: a systematic review. Clin Sarcoma Res 2020; 10: 7.
4) Shweikeh F, Bukavina L, Saeed K, Sarkis R, Suneja A, Sweiss F, Drazin D. Brain metastasis in bone and soft tissue cancers: a review of incidence, interventions, and outcomes. Sarcoma 2014; 2014: 475175.
5) Ottaviani G, Jaffe N. The epidemiology of osteosarcoma. Cancer Treat Res 2009; 152: 3-13.
6) Smeland S, Bielack SS, Whelan J, Bernstein M, Hogendoorn P, Krailo MD, Gorlick R, Janeway KA, Ingleby FC, Anninga J, Antal I, Arndt C, Brown KLB, Butterfass-Bahloul T, Calaminus G, Capra M, Dhooge C, Eriksson M, Flanagan AM, Friedel G, Gebhardt MC, Gelderblom H, Goldsby R, Grier HE, Grimer R, Hawkins DS, Hecker-Nolting S, Sundby Hall K, Isakoff MS, Jovic G, Kühne T, Kager L, von Kalle T, Kabickova E, Lang S, Lau CC, Leavey PJ, Lessnick SL, Mascarenhas L, Mayer-Steinacker R, Meyers PA, Nagarajan R, Randall RL, Reichardt P, Renard M, Rechnitzer C, Schwartz CL, Strauss S, Teot L, Timmermann B, Sydes MR, Marina N. Survival and prognosis with osteosarcoma: outcomes in more than 2000 patients in the EURAMOS-1 (European and American Osteosarcoma Study) cohort. Eur J Cancer 2019; 109: 36-50.
7) Daw NC, Chou AJ, Jaffe N, Rao BN, Billups CA, Rodriguez-Galindo C, Meyers PA, Huh WW. Recurrent osteosarcoma with a single pulmonary metastasis: a multi-institutional review. Br J Cancer 2015; 112: 278-282.
8) Chandra Gupta S, Nandan Tripathi Y. Potential of long non-coding RNAs in cancer patients: from biomarkers to therapeutic targets. Int J Cancer 2017; 140: 1955-1967.
9) Li W, Zhang L, Guo B, Deng J, Wu S, Li F, Wang Y, Lu J, Zhou Y. Exosomal FMR1-AS1 facilitates maintaining cancer stem-like cell dynamic equilibrium via TLR7/NFkappaB/c-Myc signaling in female esophageal carcinoma. Mol Cancer 2019; 18: 22.
10) Peng WX, Koirala P, Mo YY. LncRNA-mediated regulation of cell signaling in cancer. Oncogene 2017; 36: 5661-5667.
11) Fu X, Zhu X, Qin F, Zhang Y, Lin J, Ding Y, Yang Z, Shang Y, Wang L, Zhang Q, Gao Q. Linc00210 drives Wnt/beta-catenin signaling activation and liver tumor progression through CTNNBIP1-dependent manner. Mol Cancer 2018; 17: 73.
12) Li Z, Hou P, Fan D, Dong M, Ma M, Li H, Yao R, Li Y, Wang G, Geng P, Mihretab A, Liu D, Zhang Y, Huang B, Lu J. The degradation of EZH2 mediated by lncRNA ANCR attenuated the invasion and metastasis of breast cancer. Cell Death Differ 2017; 24: 59-71.
13) Raveh E, Matouk IJ, Gilon M, Hochberg A. The H19 Long non-coding RNA in cancer initiation, progression and metastasis – a proposed unifying theory. Mol Cancer 2015; 14: 184.
14) Jiang N, Wang X, Xie X, Liao Y, Liu N, Liu J, Miao N, Shen J, Peng T. lncRNA DANCR promotes tumor progression and cancer stemness features in osteosarcoma by upregulating AXL via miR-33a-5p inhibition. Cancer Lett 2017; 405: 46-55.
15) Yu X, Pang L, Yang T, Liu P. lncRNA LINC01296 regulates the proliferation, metastasis and cell cycle of osteosarcoma through cyclin D1. Oncol Rep 2018; 40: 2507-2514.
16) Kun-Peng Z, Chun-Lin Z, Xiao-Long M. Antisense lncRNA FOXF1-AS1 promotes migration and invasion of osteosarcoma cells through the FOXF1/MMP-2/-9 pathway. Int J Biol Sci 2017; 13: 1180-1191.

17) Gupta G, Chellappan DK, de Jesus Andreoli Pinto T, Hansbro PM, Bebawy M, Dua K. Tumor suppressor role of miR-503. Panminerva Med 2018; 60: 17-24.

18) Abba M, Patil N, Allgayer H. MicroRNAs in the regulation of MMPs and metastasis. Cancers (Basel) 2014; 6: 625-645.

19) Mahdian-Shakib A, Dorostkar R, Tat M, Hashemzadeh MS, Saidi N. Differential role of microRNAs in prognosis, diagnosis, and therapy of ovarian cancer. Biomed Pharmacother 2016; 84: 592-600.

20) Wang Y, Yang T, Zhang Z, Lu M, Zhao W, Zeng X, Zhang W. Long non-coding RNA TUG1 promotes migration and invasion by acting as a ceRNA of miR-335-5p in osteosarcoma cells. Cancer Sci 2017; 108: 859-867.

21) Chan JJ, Tay Y. Noncoding RNA: RNA Regulatory Networks in Cancer. Int J Mol Sci 2018; 19: 1310.

22) Long J, Xiong J, Bai Y, Mao J, Lin J, Xu W, Zhang H, Chen S, Zhao H. Construction and investigation of a lncRNA-associated ceRNA regulatory network in cholangiocarcinoma. Front Oncol 2019; 9: 649.

23) Xu M, Chen X, Lin K, Zeng K, Liu X, Xu X, Pan B, Xu T, Sun L, He B, Pan Y, Sun H, Wang S. lncRNA SNHG6 regulates EZH2 expression by sponging miR-26a/b and miR-214 in colorectal cancer. J Hematol Oncol 2019; 12: 3.

24) Li N, Zhan X. Identification of clinical trait-related lncRNA and mRNA biomarkers with weighted gene co-expression network analysis as useful tool for personalized medicine in ovarian cancer. EPMA J 2019; 10: 273-290.

25) Gautier L, Cope L, Bolstad BM, Irizarry RA. affy--analysis of Affymetrix GeneChip data at the probe level. Bioinformatics 2004; 20: 307-315.

26) Smyth GK. Linear models and empirical bayes methods for assessing differential expression in microarray experiments. Stat Appl Genet Mol Biol 2004; 3: Article3.

27) Wang H, Huo X, Yang XR, He J, Cheng L, Wang N, Deng X, Jin H, Wang N, Wang C, Zhao F, Fang J, Yao M, Fan J, Qin W. STAT3-mediated upregulation of lncRNA HOXD-AS1 as a ceRNA facilitates liver cancer metastasis by regulating SOX4. Mol Cancer 2017; 16: 136.

28) Yamamura S, Imai-Sumida M, Tanaka Y, Dahiya R. Interaction and cross-talk between non-coding RNAs. Cell Mol Life Sci 2018; 75: 467-484.

29) Benjamin RS. Adjuvant and neoadjuvant chemotherapy for osteosarcoma: a historical perspective. Adv Exp Med Biol 2020; 1257: 1-10.

30) Zhang Y, Yang J, Zhao N, Wang C, Kamar S, Zhou Y, He Z, Yang J, Sun B, Shi X, Han L, Yang Z. Progress in the chemotherapeutic treatment of osteosarcoma. Oncol Lett 2018; 16: 6228-6237.

31) Marko TA, Shamsan GA, Edwards EN, Hazelton PE, Rathe SK, Cornax I, Overn PR, Varshney J, Diessner BJ, Moriarity BS, O'Sullivan MG, Odde DJ, Largaespada DA. Slit-robo GTPase-activating protein 2 as a metastasis suppressor in osteosarcoma. Sci Rep 2016; 6: 39059.

32) Jathar S, Kumar V, Srivastava J, Tripathi V. Technological developments in lncRNA biology. Adv Exp Med Biol 2017; 1008: 283-323.

33) Li J, Meng H, Bai Y, Wang K. Regulation of lncRNA and its role in cancer metastasis. Oncol Res 2016; 23: 205-217.

34) Guo B, Wu S, Zhu X, Zhang L, Deng J, Li F, Wang Y, Zhang S, Wu R, Lu J, Zhou Y. Micropeptide CIP2A-BP encoded by LINC00665 inhibits triple-negative breast cancer progression. EMBO J 2020; 39: e102190.

35) Li W, Xie P, Ruan WH. Overexpression of lncRNA UCA1 promotes osteosarcoma progression and correlates with poor prognosis. J Bone Oncol 2016; 5: 80-85.

36) Yang Z, Li X, Yang Y, He Z, Qu X, Zhang Y. Long noncoding RNAs in the progression, metastasis, and prognosis of osteosarcoma. Cell Death Dis 2016; 7: e2389.

37) He W, Zhong G, Jiang N, Wang B, Fan X, Chen C, Chen X, Huang J, Lin T. Long noncoding RNA BLACAT2 promotes bladder cancer-associated lymphangiogenesis and lymphatic metastasis. J Clin Invest 2018; 128: 861-875.

38) Yang L, Li L, Zhou Z, Liu Y, Sun J, Zhang X, Pan H, Liu S. SP1 induced long non-coding RNA LINC00958 overexpression facilitate cell proliferation, migration and invasion in lung adenocarcinoma via mediating miR-625-5p/CPSF7 axis. Cancer Cell Int 2020; 20: 24.

39) Chitwood DH, Timmermans MC. Target mimics modulate miRNAs. Nat Genet 2007; 39: 935-936.

40) Cheng Q, Wang L. LncRNA XIST serves as a ceRNA to regulate the expression of ASF1A, BRWD1M, and PFKFB2 in kidney transplant acute kidney injury via sponging hsa-miR-212-3p and hsa-miR-122-5p. Cell Cycle 2020; 19: 290-299.

41) Liu J, Li H, Zheng B, Sun L, Yuan Y, Xing C. Competitive endogenous RNA (ceRNA) regulation network of lncRNA-miRNA-mRNA in colorectal carcinogenesis. Dig Dis Sci 2019; 64: 1868-1877.

42) Zhang G, Li S, Lu J, Ge Y, Wang Q, Ma G, Zhao Q, Wu D, Gong W, Du M, Chu H, Wang M, Zhang A, Zhang Z. LncRNA MT1JP functions as a ceRNA in regulating FBXW7 through competitively binding to miR-92a-3p in gastric cancer. Mol Cancer 2018; 17: 87.

43) Chen S, Chen JZ, Zhang JQ, Chen HX, Qiu FN, Yan ML, Tian YF, Peng CH, Shen BY, Chen YL, Wang YD. Silencing of long noncoding RNA LINC00958 prevents tumor initiation of pancreatic cancer by acting as a sponge of microRNA-330-5p to down-regulate PAX8. Cancer Lett 2019; 446: 49-61.

44) Li R, Fang L, Pu Q, Bu H, Zhu P, Chen Z, Yu M, Li X, Weiland T, Bansal A, Ye SQ, Wei Y, Jiang

J, Wu M. MEG3-4 is a miRNA decoy that regulates IL-1beta abundance to initiate and then limit inflammation to prevent sepsis during lung infection. Sci Signal 2018; 11: e2387.

45) Michishita E, Garces G, Barrett JC, Horikawa I. Upregulation of the KIAA1199 gene is associated with cellular mortality. Cancer Lett 2006; 239: 71-77.

46) Zhang Y, Jia S, Jiang WG. KIAA1199 and its biological role in human cancer and cancer cells (review). Oncol Rep 2014; 31: 1503-1508.

47) Wang XD, Lu J, Lin YS, Gao C, Qi F. Functional role of long non-coding RNA CASC19/miR-140-5p/CEMIP axis in colorectal cancer progression in vitro. World J Gastroenterol 2019; 25: 1697-1714.

48) Zhang D, Zhao L, Shen Q, Lv Q, Jin M, Ma H, Nie X, Zheng X, Huang S, Zhou P, Wu G, Zhang T. Down-regulation of KIAA1199/CEMIP by miR-216a suppresses tumor invasion and metastasis in colorectal cancer. Int J Cancer 2017; 140: 2298-2309.

49) Zhao L, Zhang D, Shen Q, Jin M, Lin Z, Ma H, Huang S, Zhou P, Wu G, Zhang T. KIAA1199 promotes metastasis of colorectal cancer cells via microtubule destabilization regulated by a PP2A/stathmin pathway. Oncogene 2019; 38: 935-949.

50) Shen F, Zong ZH, Liu Y, Chen S, Sheng XJ, Zhao Y. CEMIP promotes ovarian cancer development and progression via the PI3K/AKT signaling pathway. Biomed Pharmacother 2019; 114: 108787.